Halston Mozetic[1*], Uilian Boff[1], Wilberth H. D. Luna[2], Maiquel E. Pfingstag[3], Ricardo M. de Martins[4], Moises de M. Dias[4], Lirio Schaeffer[5]

J. Electrical Systems 12-2 (2016): 357-372

Regular paper

Journal of Electrical Systems

DEVELOPMENT OF CORES FOR MINI MOTORS FROM LAMINATED SHEETS OF ELECTRIC STEEL ABNT (Brazilian Association of Technical Standards) 35F 420M WITH THERMAL TREATMENT

The purposes of this paper were to study the thermal treatment of Fe-Si sheet, as well as the sheet cutting concerning the topology of a mini stepper motor and mini motor simulation using finite element software. The research consisted of the execution of an "Inductive Reheating" thermal treatment of Iron Silicon sheets, NM71-2000/35F 420M with GNO (Grain Non Oriented), and 0.35mm width. The new technique has the benefit of minimizing magnetic losses produced by the cut on the edge of electric sheets. To carry out the process, the system includes a furnace, an induction coil, and a power supply that, when activated in a controlled way, causes relevant changes to the crystalline structure of the material. Related to the cut of the sheets, the topology of a three phase mini stepper motor was considered. The sheets were initially cut using the geometry of the rotor and stator cores. Firstly, a die cutting process was used and later a wire electroerosion cutting process was employed, which provided parts with excellent finishing. Finally, the mini motor was simulated using the finite element software FEMM 4.2 in order to analyze the airgap flow and torque development of the axis end, in comparison to a solid block of the same material (Fe-Si).

Key Words: Sheet Thermal Treatment, sheet cutting, stepper motor, simulation using finite element methodology

Article history: Received 29 July 2015, Accepted 8 March 2016.

1. Introduction

Rotating electrical machines can function as a motor or generator and consist of two basic parts, namely the stator and rotor cores. These cores, with rare exceptions, are made from sheet metal (low carbon steel sheets) less than 1 mm thick that are stacked together. Some better performing machines, such as generators, are made from silicon steel sheets of approximately 3% silicon. The entire manufacturing process for these cores basically consists of lamination, stamping, electrical insulation between adjacent sheets, stacking and setting [1, 2].

The rotor and stator cores, depending on the configuration of the machine, are surrounded by windings powered by a sometimes alternating electric current, and are subject to the action of induced currents, also known as eddy or Foucault currents, which are responsible for appreciable power loss in these cores. The construction of these magnetic cores from electrically insulated steel sheets partially reduces eddy currents, representing the classic

* Corresponding author: E-mail halston.mozetic@ufrgs.br

[1] Centro Universitário Ritter dos Reis, Rua Orfanotrófio, 555, CEP 90840440, Porto Alegre, RS/Brasil,:

[2] Serviço Nacional de Aprendizagem Industrial (SENAI), Av. Orlando Gomes, 1845, CEP 41650010, Salvador BA/Brasil

[3] Universidade Regional Integrada do Alto Uruguai e das Missões, Campus Erechim, Av. Sete de Setembro, 1558, CEP 99700000, Erechim, RS/Brasil

[4] Instituto de Ciências Exatas e Tecnológicas, Universidade Feevale, ERS 239, 1755, CEP 93525075, Novo Hamburgo, RS/Brasil

[5] Laboratório de Transformação Mecânica (LdTM), Depto. de Metalurgia, PPGEM, Universidade Federal do Rio Grande do Sul, Av. Bento Gonçalves, 9500, CEP: 91501970, Porto Alegre, RS/Brasil

solution for minimizing eddy current losses. However, reduction of induced currents can also be achieved by increasing the electrical resistivity of the core material. In certain types of machines, permanent magnets are inserted into them in order to replace the spooling (of the rotor or stator) [1, 2].
Miniaturized motors or mini motors use the same configuration of conventional rotating machines, but with reduced dimensions. The most common of these mini motors are the stepper motor, the electrostatic motor and the direct current motor [1].
Therefore, this project was divided in three steps: thermal treatment of Fe-Si sheet, sheet cutting in the topology of a mini stepper motor, and simulation using software of finite elements of the mini motor. Concerning the thermal treatment of the sheets, this work consisted of the execution of an "Inductive Reheating" thermal treatment of silicon iron sheets, NM71-2000/ 35F 420M, GNO (Grain Non Oriented), and 0.35mm width.
Related to the cut of the sheets, the topology of a three phase mini stepper motor was considered (reluctance stepper motor) [3,4]. The sheets were initially cut using the geometry of the rotor and stator cores, and the die cutting process was employed. That process is normally used for this type of application. However, some problems happened such as warping and burring along the cutting surface of the parts. Eventually, a wire electroerosion process was used, which provided parts with excellent finishing.
Finally, the mini motor was simulated using the finite elements software FEMM 4.2 in order to analyze the airgap flow and the torque development of the axis end, in comparison to a solid block of the same material (Fe-Si).

2. ROTATING ELECTRICAL MACHINES AND MINIATURIZED MOTORS

2.1. Construction Issues that Influence the Performance of the Rotating Electrical Machines

Concerning the construction and materials used, the following factors determine the performance of the rotating electrical machines or electric motors:

- The sheets are made of ferromagnetic materials (iron or magnetic steel) since they are materials with relatively high magnetic permeability. In electrical machines, the greater the magnetic permeability of the cores, the lower the magnetic field of these cores and the greater the intensity of the airgap field. One can observe that the electromagnetic torque developed in the electric motors is proportional to the magnetic flux density in the airgap, depending on the slope of the flux lines. Therefore, stator and rotor cores of electric motors built out of materials of greater magnetic permeability result in motors with superior performance [1, 2].

- The magnetic materials of the electric machine cores should have a high level of saturation, thus allowing the machine to work with a high magnetic flux point, always below the saturation point [1, 2].

- Low carbon steel is used because this is a soft magnetic material and offers low coercivity. Loss due to hysteresis is proportional to the hysteresis cycle area, which mathematically represents the energy density. Therefore, the narrower the hysteresis cycle the lower the coercivity and the lower the level of loss due to hysteresis cycle [1, 2].

- Whenever there is the occurrence of an alternating flux over a magnetic core, there will also be the inducted currents (parasite or Foucault currents) over this core.

Both the stator and the rotor are built with laminated and insulated sheets since this insulation between sheets restricts the inducted currents to a smaller circulation area. The losses from parasite currents in a solid core are considerably larger that the losses in cores obtained from sheets with electrical insulation. The smaller the sheet width, the lower the parasite currents and the lower the loss of power in these cores. The reduction of inducted currents can also be obtained from the increase in the electrical resistance of the body, or from the increase in the electrical resistivity of the material, since resistance or resistivity and electrical current are physical quantities that are inversely proportional. Therefore, high yield electric motors are built from silicon steel sheets that offer electric resistivity that is higher that low carbon steel [1, 2].

In summary, the material used to construct the cores of the stator and rotor should present the following properties:

- high relative magnetic permeability;
- low magnetic coercivity;
- high electrical resistivity; and
- high saturation induction.

2.2. Magnetic Properties of the Cores

The magnetic properties are obtained from the hysteresis curve (Figure 1) that correlates the magnetic field **H** applied to a material with the resulting magnetic **B** induction. For the hard magnetic materials or permanent magnets, the **BxH** ratio has the characteristics demonstrated in Figure 1-(a). The hard magnetic materials such as the magnetic steels have a more narrow cycle with low coercivity. Figure 1-(b) shows graphs that compare hard with soft magnetic materials [3, 4].

The point in which the curve intercepts the B axis, in the upper left quadrant, is called remanence or remanent magnetism $\mathbf{B_r}$ and represents the residual magnetic induction that remains in the material without an applied magnetic field (H = 0). In the CGS system of units (primarily used to describe magnetic materials), **B** is given in Gauss [G]. The point where the curve intercepts the **H** axis in the same quadrant is called coercive or coercivity $\mathbf{H_C}$ and represents the magnetic field that is necessary to demagnetize the specimen (B = 0). In the CGS system, **H** has Oersted [Oe] as its unit [3, 4].

The relative magnetic permeability $\boldsymbol{\mu_r}$ is related to the highest slope point of the hysteresis curve. The saturation induction B_{max} can be seen based on the field values where the induction tends to remain constant or with an almost zero slope. The typical curve of a magnetic field is demonstrated by the solid curve of Figure 1-c. For comparison purposes, the figure shows four doted lines that correspond to the relative permeability constant $\boldsymbol{\mu}$ of 1, 10, 100 and 1000 [3, 4].

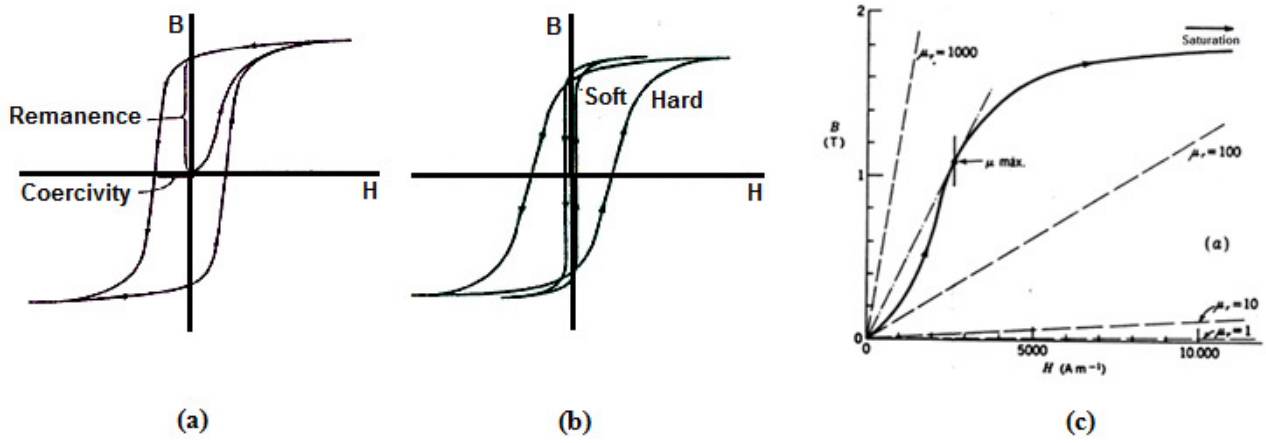

Figure 1 – Magnetic curves – (a) Hysteresis Cycle – (b) Soft and Hard magnetic materials – (c) Magnetization curve and permeability.

2.3. Physical Properties of the Sheets

The steels used for electrical purposes can be analyzed as a special class of low carbon steel with specific magnetic properties for their application in manufacturing cores for electric motors, generators, power transformers, reactors for lighting systems, energy gauges and motors for hermetic compressors on refrigerators, freezers, and air-conditioners. These steels are divided into two major families, as described in the sequence:

- grain oriented (GO) steel sheets – there is a crystallographic orientation parallel to the surface of the steel sheets. This promotes excellent magnetic properties in a single direction [5]

- grain non oriented steel sheets (GNO) - there is no preferential crystallographic orientation. The use of GNO steels is very broad, noted for its use in both small and large electric motors, lamp reactors and energy gauges.

Table 1 shows the chemical composition given by the manufacturer of the grain non oriented electric steel ABNT 35F 420M.

Table 1. Chemical composition of electric steel ABNT 35F 420M.

	Si (%)	*C (%)*	*Mn (%)*	*Al (%)*	*P (%)*	*S (%)*
ABNT 35F 420M	1.70 a 2.30	< 0.0030	< 0.060	< 0.400	< 0.0040	< 0.0080

Source: ArcelorMittal Inox Brasil [6].

Table 2 shows some typical mechanical properties of electric steel ABNT 35F420M.

Table 2. Mechanical properties of electric steel ABNT 35F 420M.

Mechanical Properties	Yield Strength (longitudinal)	Yield Strength (transversal)	Crushing Strength (longitudinal)	Crushing Strength (transversal)	Elongation (longitudinal and transversal)	Hardness
ABNT 35F 420M	300 MPa	304 MPa	420 MPa	425 MPa	30%	147 HV5

Source: ArcelorMittal Inox Brasil [6].

Electric steel is classified by ABNT guideline NM71-2000 as 35F 420M, by AISI standard M-36, by ASTM standard A677 M by 36F 195, by JIS standard 2552-2000 by 35A 360, and by standard DIN EN 10106 by M330-35A. In Brazil, the supply is exclusively from ArcelorMittal Inox Brasil that sells it under the name E-170 with a width of 0.35mm.

2.4. Thermal Treatment

The Steel and Electronic Industries, over the last few decades, have been dedicating their attention to obtain materials that meet the demand of the consumer market. One percent of the total annual steel production is used due to the magnetic properties of these materials. And of a total of approximately 7 million annual tons, 1 million are used in transformers (the so called grain oriented steels – GO), 4 million are employed in high yield electric motors, and 2 million of SAE 1006 type of steel are used for application with lower requirements [5].

In this work, a thermal treatment of the silicon steel sheets, NM71-2000/ 35F 420M, GNO (Grain Non Oriented), and 0.35mm width has been done. The low cost of the pieces as well as the facility to acquire the materials are the driven force to develop this study. The new technique employed here has the benefit of minimizing magnetic losses produced by the cut on the edge of electric sheets. These deformities strongly influence the magnetic flux due to relevant alterations caused by its cutting design. To carry out the process, the system is made up of a furnace, an induction pump, and a power source.

The reheating is mainly used in metallurgy for the relief of the remaining tension from the lamination process in order to induce the material to form a crystallographic texture of the {110} <001> type, i.e., with almost all the crystals having their planes {110} parallel to the surface with direction <001> parallel to the longitudinal direction of the material. In these conditions their magnetic properties are excellent. The main objective of the research is the search for materials with better magnetic characteristics because, with the reduction in size and the resulting reduction in magnetic losses, the yield of these machines would increase up to 36% [5].

The parameters that influence the shape of the hysteresis curve of the materials can be classified into two groups. In the first group, it can be found the intensity of the applied magnetic field and the frequency of the alternating field. In the second one, the microstructural parameters for the materials, such as microstructural differences and mismatches of the crystalline structure are the ones of interest [7]. Thus, the micro stamping and the induction field thermal treatment process were implemented on the GNO iron silicon sheets in order to improve the magnetic properties in the texture of the sheets, and more specifically in the edges of the material where the deformities were more accentuated.

2.5. Sheet Cutting

The cutting process is one of the most used separation techniques, whether in isolation, as preparation of generators for deep inlay and then excess removal, or in progressive tools that combine the cutting process with inlay and folding processes. There are several separation techniques: laser cutting, wire electroerosion and die cutting are the most used. The last one has the advantage of using a simple tool set, producing parts with adequate quality for most applications [8].
The die cutting process occurs in the following manner: when the punch tool begins to penetrate the sheet, the compressive strength converts into shearing strength (cutting strength) causing a sudden separation of a portion of the sheet. With a circular punch tool the diameter of the punch is slightly less that the diameter of the matrix so that there is a gap between them, allowing the punch penetrates the matrix, separating the plate into two parts. Figure 2 illustrates the basic components of a conventional cutting tool.

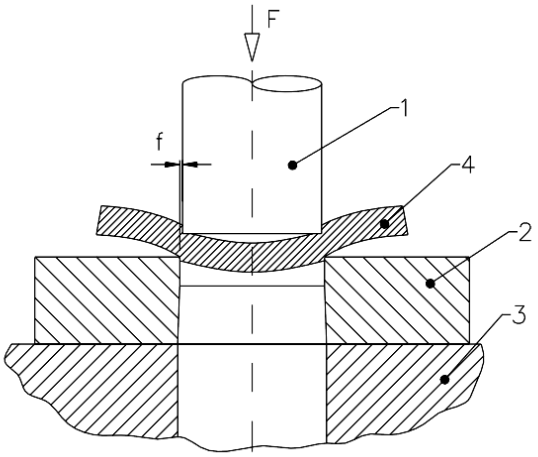

Figure 2 – Basic elements of a die cutting tool. 1- punch, 2- matrix, 3 – tool base, 4 – sheet, f – gap between punch and matrix [9].

A part obtained through the die cutting process presents its own characteristics originating from the way the tension is distributed on the sheet at the time of the cut, as seen in Figure 3. These characteristics qualitatively define the process in regards to the result of the cut.

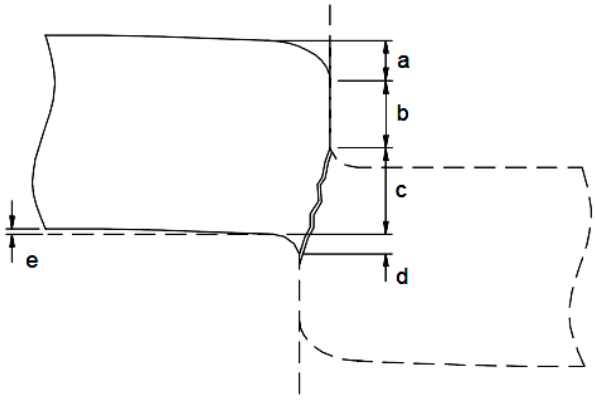

Figure 3 – Main parts of a sheared part: a- rounding zone, b – sheared zone, c- fractured zone, d- burr, e – warp [8].

2.6. Simulation Using Finite Element Software

The results of the electromagnetic iterations of a rotating electrical machine can be obtained through simulations using finite element software FEMM 4.2 (Finite Element Method Magnetics). The purpose of the finite element methodology is to solve differential equations for several entries. The main idea is to divide the problem into a large number of regions with a simple geometry (e.g. triangle). In each element, the solution is found through an interpolation of the values of each triangle vertex [9].
The advantage of dividing the initial area in small elements is based on that for a known area it is possible to resolve the problem or equation system more easily. Through the discretization process, a system of linear algebra is generated with millions of variables. The system solution occurs with the aid of processors that use algorithms that are capable of resolving the system in a short period of time. Figure 4 shows a schematic diagram regarding FEM methodology.

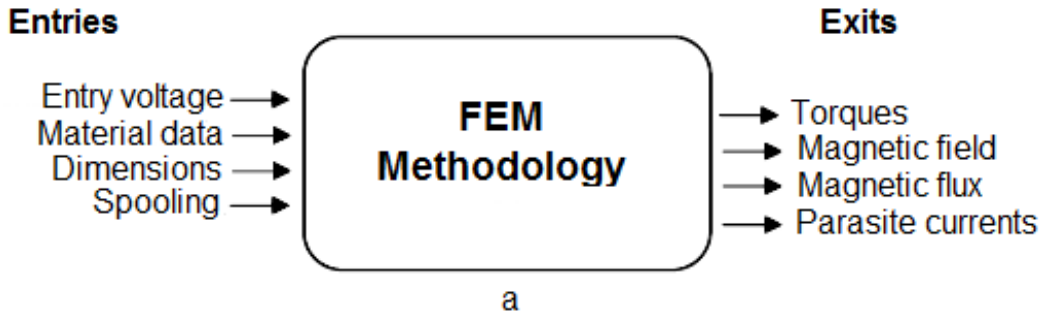

Figure 4 – FEM Methodology

FEMM 4.2 is a set of programs to resolve problems with low electromagnetic frequency in bidimensional plans with axial symmetry. The software is divided into three parts:

- **Interactive Shell**: Multiple interface with pre and post processing for various types of problems. It has a CAD (Computer Aided Design) interface for defining material properties and the limit conditions.

- **Triangle.exe**: It modifies the region to be solved in a number of triangles, a fundamental operation for the application of the finite element methodology.

- **Solvers**: Algorithm for solving magnetic and electrostatic problems. Each solution uses the configured data that describes the problem to resolve Maxwell differential equations, obtaining the values of the desired field.

By using FEMM 4.2, it is possible to verify important data such as the momentary torque of the electric machine, the flux linkage in each coil and the Foucault current losses. The knowledge of these results allows the designer to verify the efficiency of the motor and the properties that should be worked on to achieve the ideal working point.

3. MATERIAL AND METHODS

3.1. Thermal Treatment

To carry out this project, a process was developed where various samples of "thin sheets" for electrical purposes underwent a process to optimize the magnetic flux density (B) through a magnetizing force (H), resulting in a greater magnetic permeability (μ).

The main application is in electric equipment where there is an essential need to reduce loss due to the dimensions of the referred equipment. The project was based on the use of these sheets in small electric motor cores, specifically in micromotors. The application is not limited to micromotors but also to many types of equipment where the sheet cutting factor alters its electrical efficiency. As it was addressed previously, it may be used in small motors, small transformers, and lighting reactors, but also as an efficiency improvement in the power reactors, large transformers and even turbo-generators.

Based on this development, the magnetic induction process during thermal treatment was constructed. In other words, the sheets were cut and then the thermal treatment with field induction was done, as described in the following steps:

- **Step 1:** Standard sheet sized 30mm x 300mm conventional cut according to ASTM standard A343/A343M – 03/2008;

- **Step 2**: Stamping of microparts using conventional cutting according to the tool developed by Laboratório de Transformação Mecânica (LdTM)/ Universidade Federal do Rio Grande do Sul (UFRGS);

- **Step 3**: Thermal treatment using the Reheating process with Magnetic Induction (RMI), with 5 hour duration, Heraeus K 1250 Furnace, with a maximum temperature of 910°C.

The ferrosilicon sheets for the reheating and magnetic induction (RMI) thermal treatment, as shown in the graph (Figure 5), underwent the following process or procedures for the thermal treatment process with magnetic field induction using ferrosilicon sheets, ABNT NM/71-2000/35F 420 GNO (Grain Non Oriented) and 0.35 mm width:

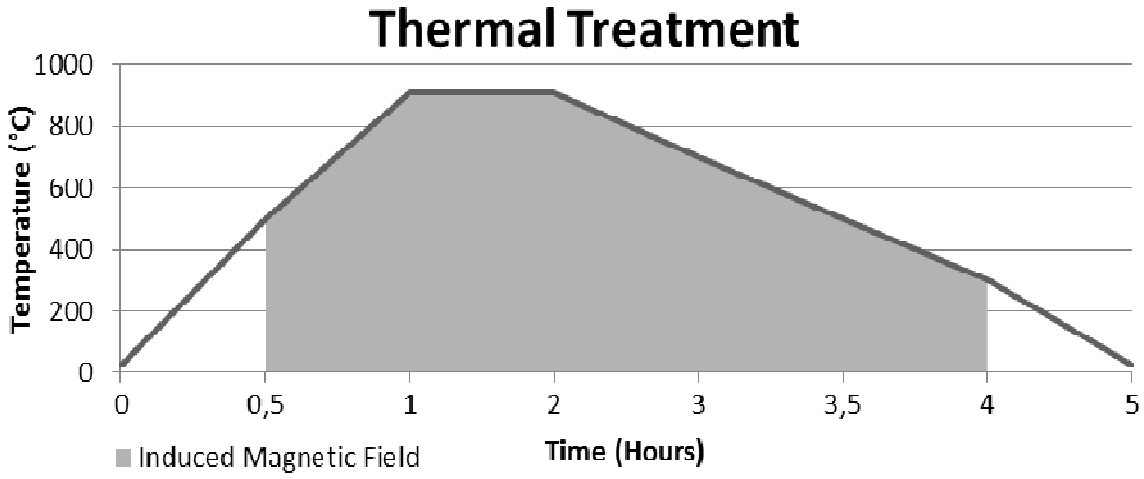

Figure 5 – Reheating and magnetic induction (RMI) thermal treatment graph.

- Heating until the austenitizing temperature, 910ºC, maintaining it in this range for 4 hours and, after cooled, returned to the furnace in 5 steps: step 1 (rate of 16 ºC/min to 500 ºC), step 2 (rate of 14 ºC/min to 910 ºC), step 3 (910 ºC/1h), step 4 (rate of 3 ºC/min of 910 ºC to 300 ºC) and step 5 (rate of 5 ºC/min of 300 ºC to room temperature, 25 ºC), characterized by the full reheating process, according to ASTM A 395 (AMERICAN SOCIETY FOR TESTING AND MATERIALS, 1993).

- During the heating process (initiating at 500ºC), an electrical current "*I*" of 20 A (Amperes) with direct voltage of 160 V (Volts), using a coil as shown in Figure 6, was applied to the system.

- At cooling, the induction current system was on until 500 ºC, when it was turned off and the system continued cooling until room temperature (for 3 hours), when the process was finished. During the simultaneous induction and reheating process, a power source was used with an entry voltage of 110V AC and exit voltage of 160 V DC, in order to obtain a current variation that is enough to fulfill the demands of the alignment of the magnetic domains.

- The maximum exit current was 20 A DC and with a maximum operational power of 3200 Watts.

- To monitor the temperature, a type K thermocouple (Chromel-Alumel) was used with an operational range from -200ºC to 1250ºC.

a) **b)**

Figure 6 – Magnetic induction current with electric current source a) Source and solenoid. b) Furnace and solenoid.
Source: (LdTM – Laboratório de Transformação Mecânica/UFRGS)

The process is extremely efficient, and the results can be seen during the alloy analysis because it presents a positive and relevant alteration concerning the crystalline structure and therefore the magnetic permeability of the material.

3.2. Cutting the Sheets of the Stepper Motor Cores

For the shearing cutting process of the strips that will be employed to construct the core of the mini motor (Figure 7), a tool was designed and built, using only conventional tool components for stamping in order to reduce the process costs.

Figure 7 shows the schematic design of the studied mini motor that had the following main characteristics:

- Stepper Motor - Variable Reluctance type;
- Stator core with three phases and two protrusions per phase, fed by pulsating DC current;
- Rotor with 4 protrusions.

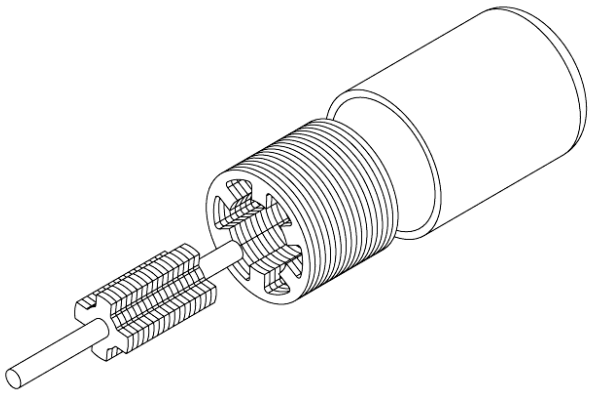

Figure 7 – Schematic design of the mini motor.

In turn, Figure 8 shows the schematic design of the cutting tool that was built. Once the sheets are very thin, the gap used between the matrix and the punch is very small, almost nonexistent, thus using only the sliding of the cutting tool for the inside of the matrix.

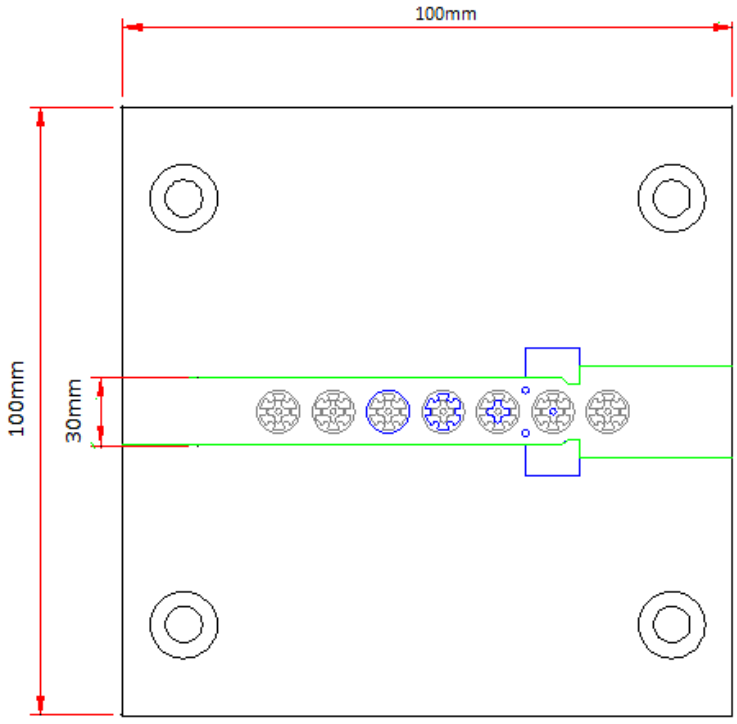

Figure 8 – Schematic design of tool used for the cutting of the rotor and stator.

The process of wire electroerosion cutting allows the materials to be cut with a fine electrode that follows a programmed path and characterized by the absence of cutting strength and tension that is common in conventional processes such as die cutting. The equipment used to make the electroerosion cut is illustrated in Figure 9, using a brass wire with 0.25mm in diameter and water lubrication.
One of the advantages of this process in comparison to die cutting is that the set can be obtained in a single step. This occurs because various sheets can be stacked together in such a way to obtain the set in a single step. The major disadvantage of this process in comparison with die cutting is its high cost as well as low productivity.

Figure 9 – Equipment used for wire electroerosion cutting [10].

3.3. Machine Simulation Aspects

The schematic mini motor shown in Figure 7 with rotor and stator cores constructed from sheets of electrical steel ABNT 35F 420M of 0.35 mm thick was simulated using the finite elements software FEMM 4.2 to analyze airgap flow and torque development of the axis end, in comparison to a solid block of the same material (Fe-Si). The characteristics of the coiling used are listed below:

- Coiling with 44 AWG gauge wire;
- Number of coils for each poles = 196 (392 per phase);
- 0.04 A Current.

Figure 10 shows the poles (protrusions) of the motor related to the phases H, I, J of the stator coils. For the simulation, the magnetization curve of the studied material was added to the software, shown in Figure 10-b. The mesh generated for the finite element simulation resulted in 21,460 elements.

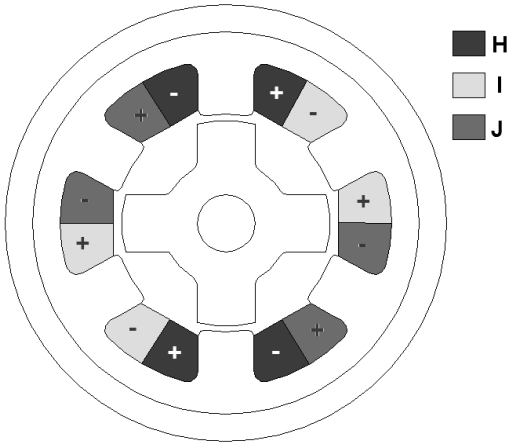

(a)

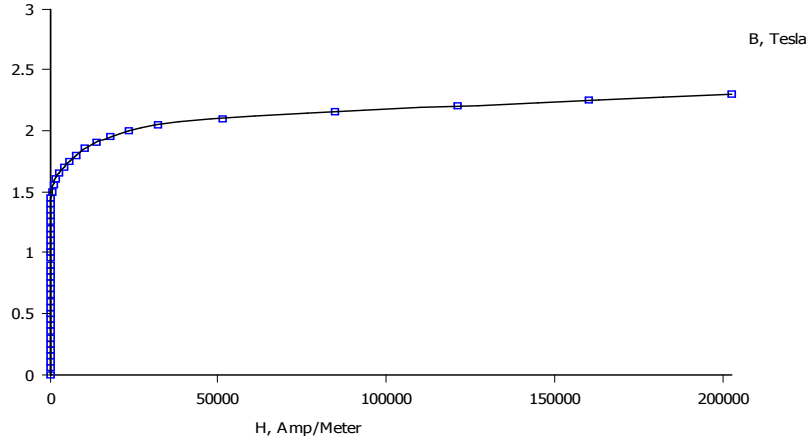

(b)

Figure 10 – Simulated Stepper Motor – (a) Configuration of the stator and rotor poles and phases H.I.J of the coil – (b) Magnetization Curve for M15 steel used for simulation

4. RESULTS AND DISCUSSIONS

4.1. Thermal Treatment

In order to obtain the relationship between the magnetic behavior and the microstructure, metallographic samples were made at LAMEF (Laboratório de Metalurgia Física at UFRGS) and at LdTM (Laboratório de Transformação Mecânica at UFRGS).
The samples observed under an optical microscope were sanded, polished, and chemically attacked with the reactant Nital 2% (2% Nitric Acid and 97% ethyl alcohol). The microscope analysis was made in the center of the cross-section of the samples and a major increase in the size of the material structural grain could be observed. The size of the grain was a major effect on the magnetic losses and there is much evidence that the coercive field is proportional to the inverse of the grain size [11, 12]. Figure 11 shows the micrography of FeSi Steel ABNT 35F 420M without thermal treatment and magnetic field induction, while the Figure 13-b shows the micrography of the same material with thermal treatment. The reheating directly influences the increase in grain size, by reducing the hysteretic losses [5].

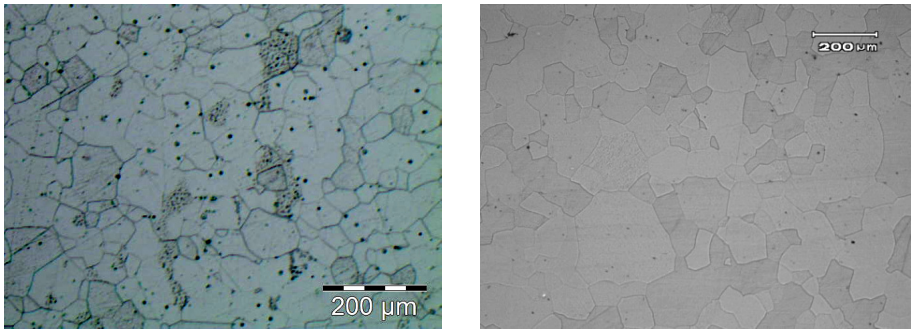

(a) **(b)**

Figure 11 – Metallography FeSi Steel ABNT 35F 420M – (a) without thermal treatment and magnetic field induction - (b) with thermal treatment.

4.2. Rotor and Stator Cores

There are several factors that can influence the magnetic performance of a motor [13, 14], but this paper only analyzes the sheet cutting process responsible for the dynamic motor losses. The strips manufactured using the die cutting process are shown in Figure 12.

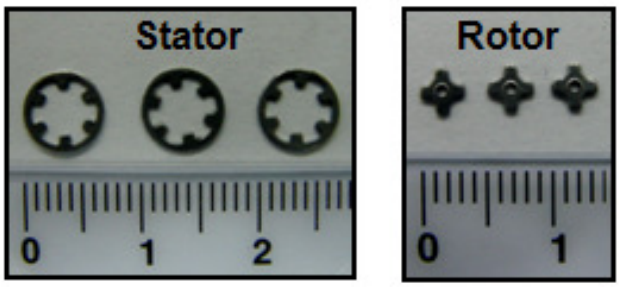

(a) **(b)**

Figure 12 – Rotor and stator strips obtained from the die cutting process – (a) Stator – (b) Rotor. Scale in centimeters.

In order to evaluate the cutting surface of the rotor and stator strips obtained from the die cutting process, a scanning electron microscope (SEM) technique was applied to the samples. Through this analysis, it was possible to analyze some typical aspects of the die cutting process, such as part warping, the emergence of burrs, deterioration, bending and the detachment of material on the cutting surface [15, 16]. Figure 13 shows how the cutting surface of the rotor and stator strip is altered by the die cutting process.

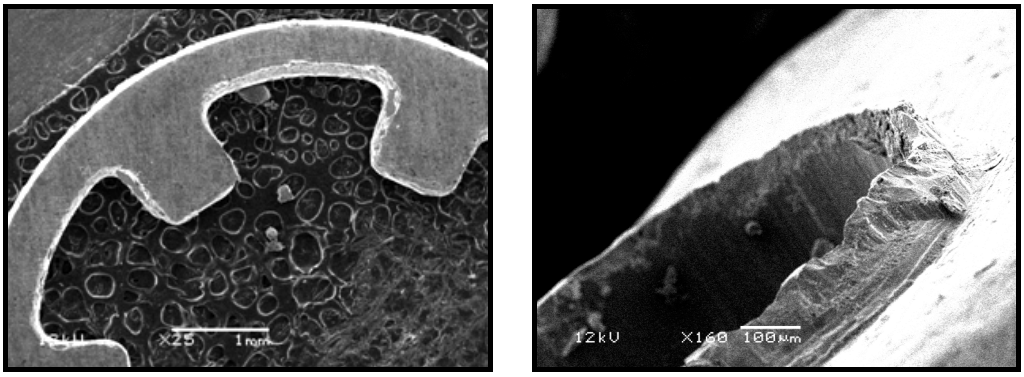

(a) **(b)**

Figure 13 – Microscopic photo of the cutting region of the rotor and stator using the die cutting process – (a) Stator – (b) Rotor**.**

In turn, Figure 14 shows the strips manufactured using the electroerosion wire cutting process. The absence of the internal perforation of the rotor is due to the fact that the diameter of the internal perforation is just 1.0 mm and once the diameter of the wire used for the process in just 0.25 mm in diameter, it was not possible to make the perforation.

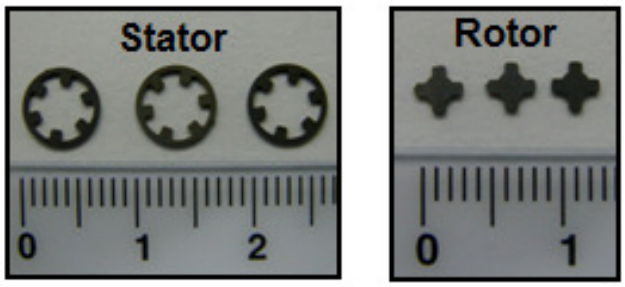

(a) **(b)**

Figure 14 – Rotor and Stator strips obtained from the electroerosion wire cutting process – (a) Stator – (b) Rotor. Scale in centimeters.

The effectiveness of this cutting process can be seen through an analysis by SEM where the cutting surfaces of the rotor and stator strips are presented (Figure 15). The images show that the electroerosion wire cutting process provided smooth surfaces, with no imperfections – in contrast to the die cutting process.

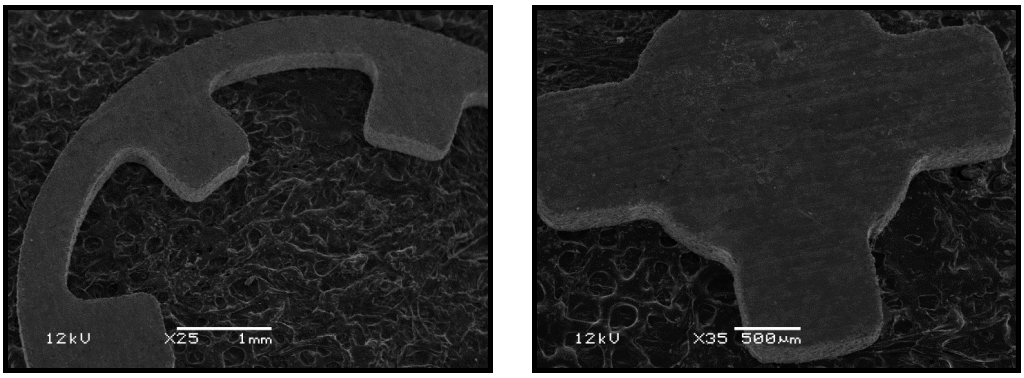

(a) **(b)**

Figure 15 – Microscopic photo of the cutting region of the rotor and stator using the electroerosion wire cutting process – (a) Stator – (b) Rotor.

4.3. Simulation Results

Figure 16-a shows the magnetic flux density of the airgap in Tesla and Figure 16-b presents the flux lines generated inside the machine.

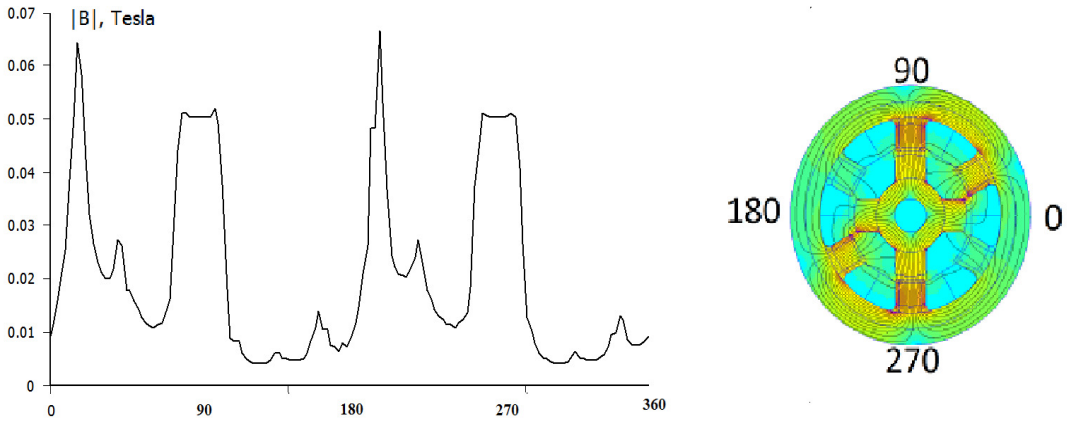

(a) **(b)**

Figure 16 – Flux density in airgap - (a) Tesla Graph - (b) Flux lines inside the machine

The FEMM 4.2 Software also calculated the resulting torque and the co-energy of the magnetic field, listed below:

- **Torque (Sheets) = 0.9018** gf*mm (with a packaging factor of 0.58 – the packaging factor depends on the layer of insulation between the sheets. A value equal to 1 would be perfect, which means a spacing between the sheets equal to zero.

- **Torque (Solid Block) = 0.9068** gf*mm (same material Fe-Si as the sheets – packaging factor equal to 1)

- **Co-energy of Magnetic Field =** 1.6879 Joule.

5. CONCLUSIONS

Observing the results obtained from optical microscope images of the center of the cross-section of the samples, a large increase can be seen in the grain size of the material structure of the FeSi Steel ABNT 35F 420M with thermal treatment. Under these conditions, the magnetic properties of the samples are excellent. It can be inferred that the size of the enlarged grain significantly improves the magnetic performance of the sheets, since the microstructural differences and the discrepancies in the crystalline structure are minimized, especially on the sheet edges where the deformities are more determining.
Based on the results obtained using a scanning electron microscope, it was proven that the die cutting process for this specific case should not be applied due to the quantity of imperfections that resulted from the process on the cutting surface of the strips. The electroerosion wire cutting process, however, provided parts with excellent finishing, without the presence of burrs, free from warping or any other imperfection, and is the most recommended method for this case.
The simulation of the motor with electric steel sheets ABNT 35F 420M was compared to the motor with a solid core (without the use of sheets but considering the same Fe-Si material). The torque of the sheet motor was 0.56% lower compared to the motor torque of solid cores. The packaging factor of the used sheets was 0.58 (a value of 1 means that there is no space between the sheets). This characteristic is extremely important because in an ideal motor, if there were no problems with eddy or Foucault currents, it would be built out

of solid blocks because it would generate more torque [1,2]. In other words, this sheet cutting results in a motor with solid core torque characteristics without the undesired characteristics of parasite currents

Acknowledgment

The authors would like to thank FAPERGS and CNPq for funding this research, as well as LAMEF (Laboratório de Metalurgia Física from UFRGS) and LdTM (Laboratório de Transformação Mecânica from UFRGS).

References

[1] S.A. Nasar. *Handbook of Electric Machines*. New York, McGraw-Hill, 1987.
[2] A.E. Fitzgerald; C. Kingsley Jr.; S.D. Umans. *Electric Machinery*. New York, McGraw-Hill Inc, 599p. 1990.
[3] D. Jiles. *Introduction to Magnetism and Magnetic Materials*. London, Chapman and Hall, 440p., 1991.
[4] J.D. Kraus; K.R. Carver. *Eletromagnetismo*. Rio de Janeiro, Guanabara, 780p., 1978.
[5] F.J.G. Landgraf. *Propriedades Magnéticas de aços para fins elétricos*. In: Ivani Bott; Paulo Rios; Ronaldo Paranhos. (Organizadores.). Aços: perspectivas para os próximos 10 anos. 1ª ed. Rio de Janeiro/RJ, Brasil, 109-128, 2002.
[6] ArcelorMittal Inox Brasil. *Catálogo dos aços elétricos*. www.arcelormittalinoxbrasil.com.br. Accessed on 6th, march 2012.
[7] W.D. Callister Jr & D.G. Rethwisch. *Materials Science and Engineering: an Introduction*. 7th. ed. New York: John Wiley & Sons, 975p. 2006.
[8] J.H.C. Souza. *Estudo do processo de corte de chapas por cisalhamento*. Dissertação de mestrado. PPGEM – UFRGS, Porto Alegre, RS, Brasil, 65p. 2001.
[9] D. Meeker. *Finite Element Method Magnetics.* User's Manual, v.4.2, 2010.
[10] FANUC. *Catálogo de produtos Fanuc Robocut α-oiE/α-1iE*, 2010.
[11] H. Shimanaka; Y. Ito; K. Matsumara; B. Fukuda. Recent development on non-oriented electrical steel sheets. *Journal of Magnetism and Magnetic Materials*, 26 (1-3), 57-64, 1982.
[12] G. Bertotti; G. Di Schino; A.F. M.F. Fiorillo. On The Effect of Grain Size on Magnetic Losses of 3% Non-Oriented SiFe, *Journal de Physique Colloques*, 9, C6-385-C6-388, 1985.
[13] G. Bertotti. Eddy Currents (Chapter 12) In *Hysteresis in Magnetism*, pp. 391-430, 1998.
[14] G. Bertotti. Hysteresis in Preisach Systems (Chapter 14) In *Hysteresis in Magnetism*, pp. 479-506, 1998.
[15] M.A. Magella; R.V.B.D. Torre; I. Kühn. Estudo no comportamento ao cisalhamento de aços para fins elétricos – Parte 1: Caracterização mecânica**.** *CONAMET/SAM – SIMPÓSIO MATÉRIA*, 2002.
[16] M.A. Magella; R.V.B.D.; I. Kuhn. Estudo no comportamento ao cisalhamento de aços para fins elétricos – Parte 2: Caracterização microestrutural. *SIMPÓSIO MATÉRIA*, 2002.